Elucidation of the neurological effects of clothianidin exposure at the no-observed-adverse-effect level (NOAEL) using two-photon microscopy in vivo imaging

Nishi, Misaki ; Sugio, Shouta ; Hirano, Tetsushi ; Kato, Daisuke ; Wake, Hiroaki ; Shoda, Asuka ; Murata, Midori ; Ikenaka, Yoshinori ;…

(Citation)
Journal of Veterinary Medical Science,84(4):585-592

(Issue Date)
2022-04

(Resource Type)
journal article

(Version)
Version of Record

(URL)
https://hdl.handle.net/20.500.14094/90009430

The Journal of Veterinary Medical Science

NOTE

Toxicology

Elucidation of the neurological effects of clothianidin exposure at the no-observed-adverse-effect level (NOAEL) using two-photon microscopy *in vivo* imaging

Misaki NISHI[1)], Shouta SUGIO[3)], Tetsushi HIRANO[4)], Daisuke KATO[3)], Hiroaki WAKE[3)], Asuka SHODA[1)], Midori MURATA[1)], Yoshinori IKENAKA[5-8)], Yoshiaki TABUCHI[4)], Youhei MANTANI[2)], Toshifumi YOKOYAMA[1)] and Nobuhiko HOSHI[1)]*

[1)]Laboratory of Animal Molecular Morphology, Department of Animal Science, Graduate School of Agricultural Science, Kobe University, Hyogo, Japan
[2)]Laboratory of Histophysiology, Department of Animal Science, Graduate School of Agricultural Science, Kobe University, Hyogo, Japan
[3)]Department of Anatomy and Molecular Cell Biology, Graduate School of Medicine, Nagoya University, Aichi, Japan
[4)]Life Science Research Center, University of Toyama, Toyama, Japan
[5)]Laboratory of Toxicology, Department of Environmental Veterinary Sciences, Faculty of Veterinary Medicine, Hokkaido University, Hokkaido, Japan
[6)]Translational Research Unit, Veterinary Teaching Hospital, Faculty of Veterinary Medicine, Hokkaido University, Hokkaido, Japan
[7)]One Health Research Center, Hokkaido University, Hokkaido, Japan
[8)]Water Research Group, Unit for Environmental Sciences and Management, North-West University, Potchefstroom, South Africa

J. Vet. Med. Sci.
84(4): 585–592, 2022
doi: 10.1292/jvms.22-0013

Received: 11 January 2022
Accepted: 18 February 2022
Advanced Epub:
10 March 2022

ABSTRACT. Neonicotinoid pesticides (NNs) cause behavioral abnormalities in mammals, raising concerns about their effects on neural circuit activity. We herein examined the neurological effects of the NN clothianidin (CLO) by *in vivo* Ca^{2+} imaging using two-photon microscopy. Mice were fed the no-observed-adverse-effect-level (NOAEL) dose of CLO for 2 weeks and their neuronal activity in the primary somatosensory cortex (S1) was observed weekly for 2 weeks. CLO exposure caused a sustained influx of Ca^{2+} in neurons in the S1 2/3 layers, indicating hyperactivation of neurons. In addition, microarray gene expression analysis suggested the induction of neuroinflammation and changes in synaptic activity. These results demonstrate that exposure to the NOAEL dose of CLO can overactivate neurons and disrupt neuronal homeostasis.

KEYWORDS: clothianidin, neonicotinoid, neurotransmission, two-photon calcium imaging

Neonicotinoid pesticides (NNs) are novel neuroactive insecticides with nicotine-like structures, which were first registered in the early 1990s. There are three main characteristics of NNs. First, NNs have *selective toxicity*: their affinity for insects is tens to hundreds of times higher than that of mammalian nicotinic acetylcholine receptors (nAChRs), and they exert their insecticidal effects by inducing sustained neuronal excitation of insect nAChRs [37]. Second, their effects are *systemic*: NNs are water-soluble and absorbed through the roots and leaves of crops, and thus exert insecticidal effects on the crops themselves [32]. And third, their effects are *persistent*: NNs remain in soil and water for a long time [32]. As a result of these attractive characteristics, and their relative safety and convenience, NNs have been widely used around the world since the beginning of the 21st century as alternatives to organophosphorus pesticides, which are highly toxic to mammals.

In recent years, however, it has become clear that NNs have agonistic effects on mammalian nAChRs [16]. In addition, desnitro-imidacloprid, a metabolite of the insecticide imidacloprid, a type of NN, is highly toxic to mice and potentially other mammals due to a dramatic shift from insect-selective to vertebrate-selective action and its interaction with cerebral α4β2 nAChRs [4, 36]. Clothianidin (CLO), the NN studied herein, also forms desmethyl-CLO by demethylation. Moreover, CLO forms not only

*Correspondence to: Hoshi, N.: nobhoshi@kobe-u.ac.jp, Laboratory of Animal Molecular Morphology, Department of Animal Science, Graduate School of Agricultural Science, Kobe University, 1-1 Rokkodai, Nada, Kobe, Hyogo 657-8501, Japan

desmethyl-CLO but also desnitro-CLO by reduction of the nitro group [25]. Hence, the toxicity of the metabolites of CLO as well as imidacloprid is of concern. More recently, it has been shown to have neurobehavioral effects in mammals even below the no-observed-adverse-effect-level (NOAEL) doses [10–13, 20, 33, 34, 39]. In addition, a correlation has been found between pesticide use and an increase in developmental disorders such as autism and learning disabilities [3, 27]. NNs have been detected in urine of newborns [14, 28], in children living around NNs sprayed areas [15] and in breast milk [5], and the significant increase in NN concentrations in human urine between 1994 and 2011 [38] has raised concerns about the effects of these agents on higher brain functions and neural circuit activity in mammals, including humans.

In the mammalian brain, α4β2- and α7-type nAChRs are widely present, and these receptors are involved in anxiety and fear [30], learning memory [19], brain development [29], and the development of monoaminergic neural circuits such as those involving dopamine and serotonin [6]. In fact, our previous reports showed that a single administration of CLO to mice increased anxiety-like behavior and the number of c-fos positive cells in the paraventricular nucleus of the thalamus and the hippocampus [10, 11]. In addition, other previous studies have reported that local injection of CLO to the striatum causes transient dopamine release [8] and that exposure to acetamiprid and imidacloprid *in vitro* causes Ca^{2+} influx into neurons [16]. These findings suggest that exposure to NNs induces transient neuronal excitation via α4β2 and α7 nAChRs, leading to emotional changes. However, it is difficult to investigate dynamic changes in neuronal activity in mice exposed to NNs using conventional methods, and it is not clear what mechanism is responsible for the emotional changes induced by exposure to NNs.

In this study, we examined the dynamic changes of neural activity in the brains of awake mice exposed to CLO for 2 weeks using *in vivo* fluorescence Ca^{2+} imaging with a two-photon microscope [22]. This imaging modality is a new tool for observing the inside of living tissues and organs and analyzing the dynamics of living cells and molecules in real time, and in our study we used it for the first time to examine the dynamic changes in neural activity caused by repeated exposure to CLO. We also focused on comprehensive gene expression changes, and performed microarray analysis.

C57BL/6J male mice (6 weeks old) were purchased from Japan SLC (Hamamatsu, Japan) and were maintained in individual ventilated cages (Sealsafe Plus Mouse IVC Green Line 2GM140; Tecniplast, Buguggiate, Italy) under controlled temperature (23 ± 2°C) and humidity (50 ± 10%) on a 14-hr light/10-hr dark cycle at the Kobe University Life-Science Laboratory with *ad libitum* access to a pellet diet (DC-8; Clea Japan, Tokyo, Japan). This study was approved by the Institutional Animal Care and Use Committee (Permission #30-01-01) and was carried out according to the Kobe University Animal Experimentation Regulations.

Individuals used for two-photon Ca^{2+} imaging underwent brain surgery at 6–7 weeks of age [1, 26]. Under anesthesia with ketamine (74 mg/kg, *i.p.*) and xylazine (10 mg/kg, *i.p.*), the parietal skin was shaved and disinfected with 70% (w/vol) ethanol, and a surface anesthetic (Xylocaine jelly; Sandoz, Tokyo, Japan) was applied to the head. The skin was then cut open to expose the skull and washed. A custom-made head plate was bonded to the skull with dental cement (Fujilute BC; GC, Bistite II; Tokuyama Dental, Tokyo, Japan). The surface of the skull was coded with acrylic dental adhesive resin cement (Super Bond; Sun Medical, Moriyama, Japan) to prevent drying. Mice were allowed to recover for one day before craniotomy and virus injection. The next day, under isoflurane (1%) anesthesia, a circular craniotomy (2 mm in diameter) was performed on the left primary somatosensory cortex (S1) (centered at 1.5 mm posterior and 2.5 mm lateral from the bregma) using a dental drill [21]. After craniotomy, a glass pipette (DGC-1; Narishige, Tokyo, Japan) with a tip diameter of 10 µm was used to inject an adeno-associated virus vector (AAV vector) in the S1 layers 2/3 (L2/3) (Fig. 1A). An AAV vector, AAV1-hSyn-GCaMP6f (Addgene; 1.0×10^{12} vector genomes/ml), which expresses a neuron-specific fluorescent calcium indicator protein (GCaMP6f), was injected at a total pressure of 1 µl at three sites at a depth of approximately 200 to 300 µm from the cortical surface (Fig. 1B). After injection, a custom-made circular cover glasses (Matsunami Glass Co., Osaka, Japan) was placed on the brain surface, bonded with UV-curing adhesive (NOR-61; Norland Products, Cranbury, NJ, USA), and then the edges of the cranial window were sealed with dental cement and acrylic dental adhesive resin cement to create an observation window. The *in vivo* fluorescence Ca^{2+} imaging was started about 3–4 weeks after the surgery (9–11 weeks of age).

Two-photon microscopy (water immersion objective: ×10, XLPlan, NA 1.0, Zeiss, Tokyo, Japan; microscope: LSM 7 MP, Zeiss; titanium sapphire laser: Mai Tai HP, Spectra-Physics, Santa Clara, CA, USA) was used for Ca^{2+} imaging in the L2/3 of the left S1 (Fig. 1A). Ca^{2+} imaging of neurons in the L2/3 of the left S1 was performed. The imaging area was 512 × 512 pixels (848.54 µm ×848.54 µm), and the depth was 150–200 µm from the cortical surface. The pixel size was 1.657 µm and the frame time was 390 msec. Three consecutive imagings of 1,000 frames each were performed for each imaging session. A total of three observations were performed every week starting from the day of administration (Fig. 1B).

The analysis of the images was performed using ImageJ (National Institutes of Health, Bethesda, MD, USA) and programs created in MATLAB® R2019b (The MathWorks, Natick, MA, USA). TurboReg, introduced in ImageJ, was used to correct the displacement of the focal plane of the images [35]. To quantify neural activity in S1, regions of interests (ROIs) around cells showing fluorescence changes were visually determined during the imaging phase (Fig. 2A, 2H). Ca^{2+} responses were detected when the fluorescence intensity exceeded two standard deviations (SD) from the mean of the reference value. Ca^{2+} waveform values were used to measure the frequency and amplitude (Peak-Amplitude) of Ca^{2+} transients, the cross-correlation (C.C.) of neuronal populations, and the area under the curve (AUC) (Fig. 2B, 2I).

CLO of 95% purity was generated from Dantotsu (containing 16% CLO; Sumitomo Chemical, Tokyo, Japan) [10]. With reference to the NOAEL dose (C57BL/6J male mice: 47.2 mg/kg/day [9]), the mice were divided into two groups: a control group (0 mg/kg/day, n=5) and a CLO group (50 mg/kg/day, n=7). To avoid the influence associated with forced oral administration, mice were given a water supply gel (MediGel® Sucralose; ClearH_2O, Portland, ME, USA) with CLO or vehicle (1% dimethyl sulfoxide: DMSO) for 2 weeks.

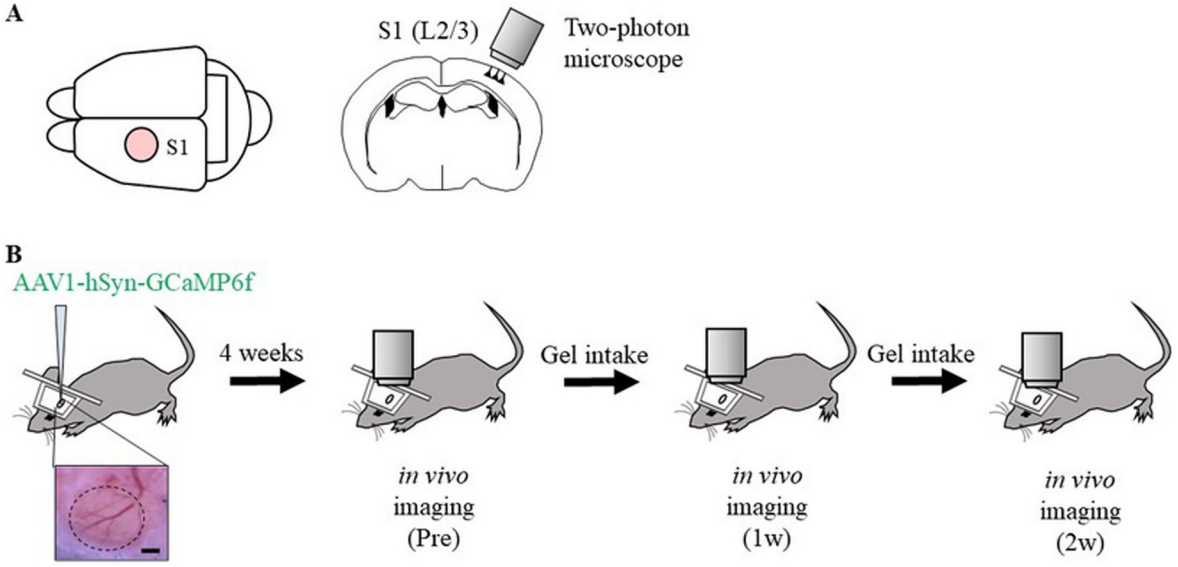

Fig. 1. A schematic drawing of the experimental procedure for the two-photon microscopy. (**A**) Schematic of L2/3 of the primary somatosensory cortex (S1) imaged by two-photon microscopy. (**B**) Schematic of virus injection, administration period, and timing of imaging. In wild-type mice, AAV1-hSyn-GCaMP6f encoding GCaMP6 was injected into L2/3 of S1 to enable *in vivo* Ca^{2+} imaging of neurons. Gel administration was started approximately 4 weeks after injection. Responses from the same neurons were followed before (Pre), 1 week (1w), and 2 weeks (2w) after clothianidin injection. Scale bar: 500 µm.

In place of the calcium imaging analysis, 6 animals per group were treated with CLO for 2 weeks and used exclusively for microarray analysis. The brain was removed and sliced into 2 mm thick slices using a brain slicer (Muromachi Kikai, Tokyo, Japan), and the S1 was cut out under visual observation. Total RNA was extracted using a NucleoSpin® RNA Plus (Macherey-Nagel GmbH & Co., Düren, Germany) according to the manufacturer's instructions. The final step, RNA extraction from the column, was performed twice with 30 µl of nuclease free water, and the concentration was measured at 260 nm absorbance using a NanoDrop 2000 (Thermo Fisher Scientific, Waltham, MA, USA) and stored at −80°C until use.

RNA quality was analyzed using a Bioanalyzer 2100 and RNA6000 Nano LabChip kit (Agilent Technologies, Santa Clara, CA, USA), and samples with a RIN (RNA integrity number) value of 7.0 or higher were used for microarray analysis (Control group: n=2; CLO group: n=2). Total RNA (250 µg) from each sample was amplified and labeled using a GeneChip WT PLUS Reagent Kit, and hybridized with a Clariom™ S mouse array (Affymetrix, Santa Clara, CA, USA). All microarrays were washed and stained with a GeneChip Hybridization, Wash, and Stain Kit and GeneChip Fluidics Station 450, and scanned with a GeneChip Scanner 3000 (Affymetrix). The raw data were normalized by the SST-RMA algorithm using Transcriptome Analysis Console software (Thermo Fisher Scientific). The data were analyzed using the Ingenuity Pathways Analysis (IPA) tool (Ingenuity Systems, Mountain View, CA, USA) to investigate the molecular function of the variable expression genes. The microarray data (.CEL files) have been deposited in a public database (Gene Expression Omnibus; accession number: GSE193245).

Statistical analysis was performed using Excel Statistics 2012 for Windows (Version 1.00; SSRI, Tokyo, Japan). For each measurement result, the Friedman test was used; a *P*-value of <0.05 was considered significant.

The measured values of Ca^{2+} transient frequency, C.C., Peak-Amplitude, and AUC are summarized in Table1. Two-photon Ca^{2+} imaging analysis showed that the frequency of Ca^{2+} transients, C.C., Peak-Amplitude, and AUC were not significantly different in the control group at each time point (Fig. 2C–G). In contrast, the frequency of Ca^{2+} transients in the CLO group was significantly decreased after 1 and 2 weeks of treatment (Fig. 2K). The Peak-Amplitude showed an increasing trend after 1 week of treatment, and AUC increased significantly after 1 and 2 weeks of treatment (Fig. 2M, 2N). In addition, there was a moderate inverse correlation between the frequency of Ca^{2+} transients and AUC in the CLO group, suggesting that the sustained influx of Ca^{2+} reduced the frequency of Ca^{2+} transients (Fig. 3).

Eighty percent of the neurons in L2/3 of the cortex are pyramidal cells, and nAChRs are present only in interneurons [31]. In addition, α7 nAChR, for which CLO has affinity, is expressed in somatostatin interneurons and parvalbumin interneurons, and β2 nAChR is only expressed in somatostatin interneurons [17]. In addition, it has been reported that pyramidal cells are activated in α7 and β2 nAChR-deficient mice and that chronic nicotine exposure desensitizes somatostatin interneurons and activates pyramidal cells [17]. Therefore, the present study showed that CLO exposure at the NOAEL dose may have activated pyramidal cells by desensitizing nAChRs expressed in interneurons. In our previous study, the number of c-fos positive cells, an index of neuronal activity, increased in the paraventricular nucleus of the thalamus and the hippocampus after a single [11] or repeated (data not shown) administration of CLO to mice, and anxiety-like behavior was also observed after a single or chronic administration [10, 11]. Therefore, the overactivity of pyramidal cells in this study may be one of the mechanisms that induce anxiety-like behavior.

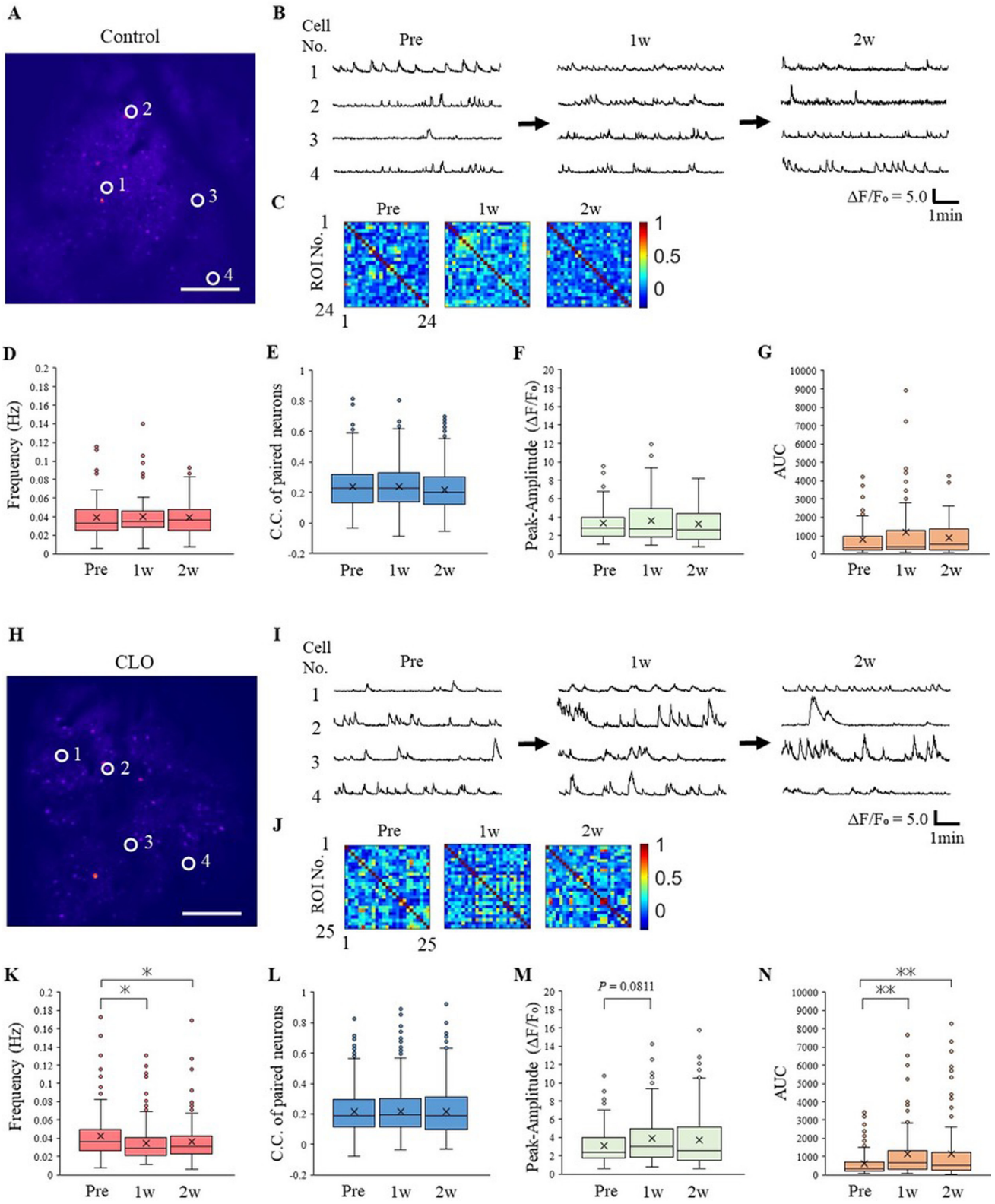

Fig. 2. Neuronal activity in the control group and clothianidin (CLO) group. (**A**, **H**) Representative images of GCaMP6f-expressing neurons. Cells showing representative Ca^{2+} responses before and after treatment are circled. Scale bar: 100 µm. (**B**, **I**) Calcium waveforms of four representative neurons in the control group at before (Pre), 1 week (1w), and 2 weeks (2w) after administration. (**C**, **J**) Representative results of correlation coefficients of paired Ca^{2+} responses from the same neuron. (**D**, **K**) Frequency of Ca^{2+} transients before and after administration. (**E**, **L**) Cross-correlation of neuronal populations. (**F**, **M**) Amplitude of the Ca^{2+} waveform before and after administration. (**G**, **N**) Area under the Ca^{2+} waveform. (Control group: n=73, 5 animals; CLO group: n=129, 7 animals) **P*<0.05, ***P*<0.01.

Table 1. Summary of the neuronal activities in the primary somatosensory cortex

	Control			
	Frequency (Hz)	C.C. of paired neuron	Amplitude ($\Delta F/F_0$)	AUC
Pre	0.0384 ± 0.0030	0.238 ± 0.0054	3.35 ± 0.24	795 ± 109
1w	0.0402 ± 0.0025	0.238 ± 0.0055	3.56 ± 0.27	1,188 ± 194
2w	0.0394 ± 0.0023	0.219 ± 0.0050	3.25 ± 0.23	901 ± 110
	CLO			
	Frequency (Hz)	C.C. of paired neuron	Amplitude ($\Delta F/F_0$)	AUC
Pre	0.0428 ± 0.0024	0.214 ± 0.0035	3.12 ± 0.18	596 ± 55
1w	0.0344 ± 0.0018*	0.218 ± 0.0035	3.93 ± 0.24	1,150 ± 130**
2w	0.0359 ± 0.0020*	0.215 ± 0.0038	3.74 ± 0.27	1,130 ± 140**

C.C.: cross-correlation, AUC: area under the curve. Mean ± SE, n=5–7. *P<0.05, **P<0.01: *vs.* Pre. Responses from the same neurons were followed before (Pre), and 1 week (1w) and 2 weeks (2w) after CLO (clothianidin) administration.

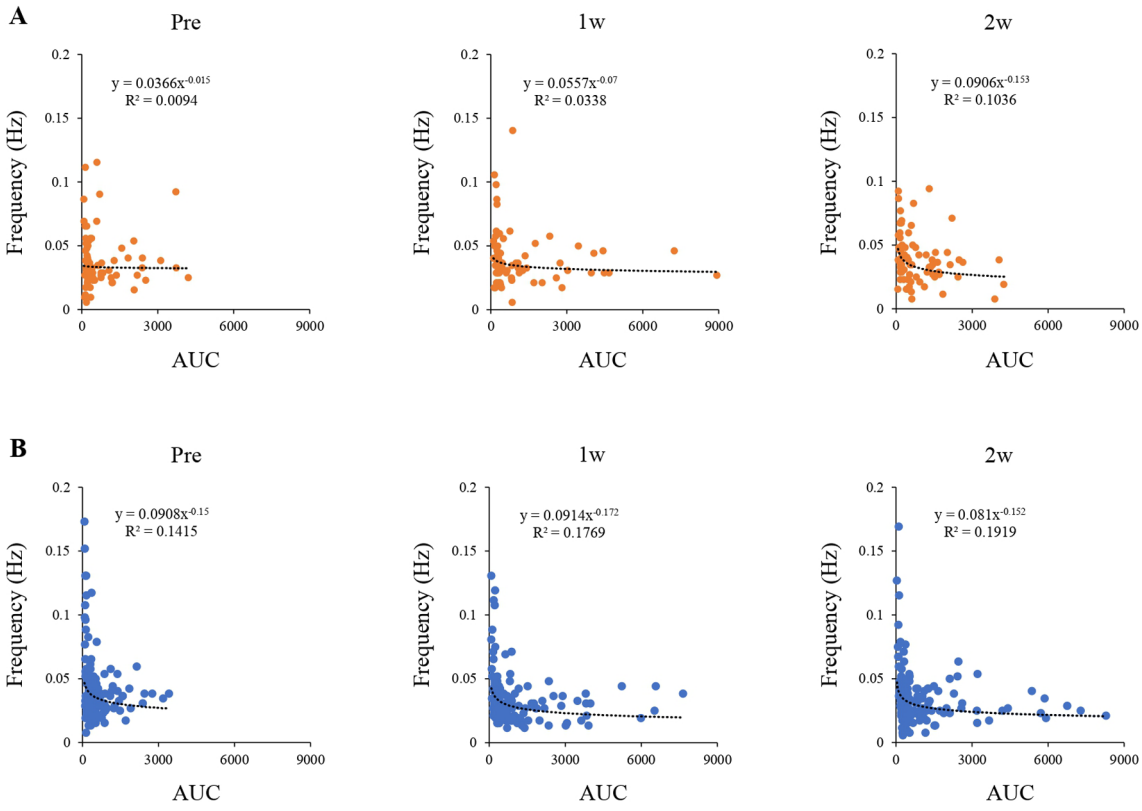

Fig. 3. Scatter plot of correlative changes in area under the Ca^{2+} waveform (AUC) and frequency of Ca^{2+} transients in the control group (**A**) and the clothianidin (CLO) group (**B**).

To further understand the mechanism of the effect of CLO on S1, we performed transcriptome analysis using the Clariom™ S mouse array and identified 677 up-regulated and 838 down-regulated genes that were more than 1.5-fold altered in the CLO group compared to the control group. The main genes whose expression increased or decreased are summarized in Table 2. Bioinformatics analysis focusing on neural functions revealed a molecular network associated with "inflammation of the central nervous system" and "cell death of cerebral cortical cells" in the 677 up-regulated genes (Fig. 4A). The increase of *TLR2* in this study is consistent with the results of a previous report in which imidacloprid was administered chronically [7]. The cerebral microglia are responsible for immune function that induces inflammation via TLR2 expression [24]. CLO exposure may have affected not only neurons but also microglia. Fetal exposure to CLO has been reported to decrease the number of microglia and decrease the ability to eat in 10-day-old mice [23]. However, the effect of CLO on microglia in adult mice is still unknown. Therefore, it will be necessary to investigate the effect of CLO on microglia in the future. On the other hand, molecular networks associated with "cortical cell death", "progressive neuropathy", and "synaptic transmission" were found in the 838 down-regulated genes (Fig. 4B). *CHAT*, which is involved in the synthesis of acetylcholine, and *ACHE*, which is involved in its degradation, as

Table 2. Major variable genes involved in neural function

Symbol	Entrez gene name	*P*-value	Expression fold change	Expected
FASLG	Fas ligand	0.0043	1.90	Up
GABRG1	Gamma-aminobutyric acid type A receptor subunit gamma1	0.0030	2.16	Up
TICAM1	Toll like receptor adaptor molecule 1	0.0081	1.89	Up
TLR2	Toll like receptor 2	0.0155	1.68	Up
CHRNA7	Cholinergic receptor, nicotinic, alpha polypeptide 7	0.0202	−1.73	Down
ACHE	Acetylcholinesterase	0.0273	−1.81	Down
SERPInNA3N	Serine (or cysteine) peptidase inhibitor, clade A, member 3N	0.0103	−2.15	Down
CHAT	Choline acetyltransferase	0.0298	−1.55	Down
PSEN1	Presenilin 1	0.0392	−1.57	Down
GABRP	Gamma-aminobutyric acid (GABA) A receptor, pi	0.0119	−1.80	Down

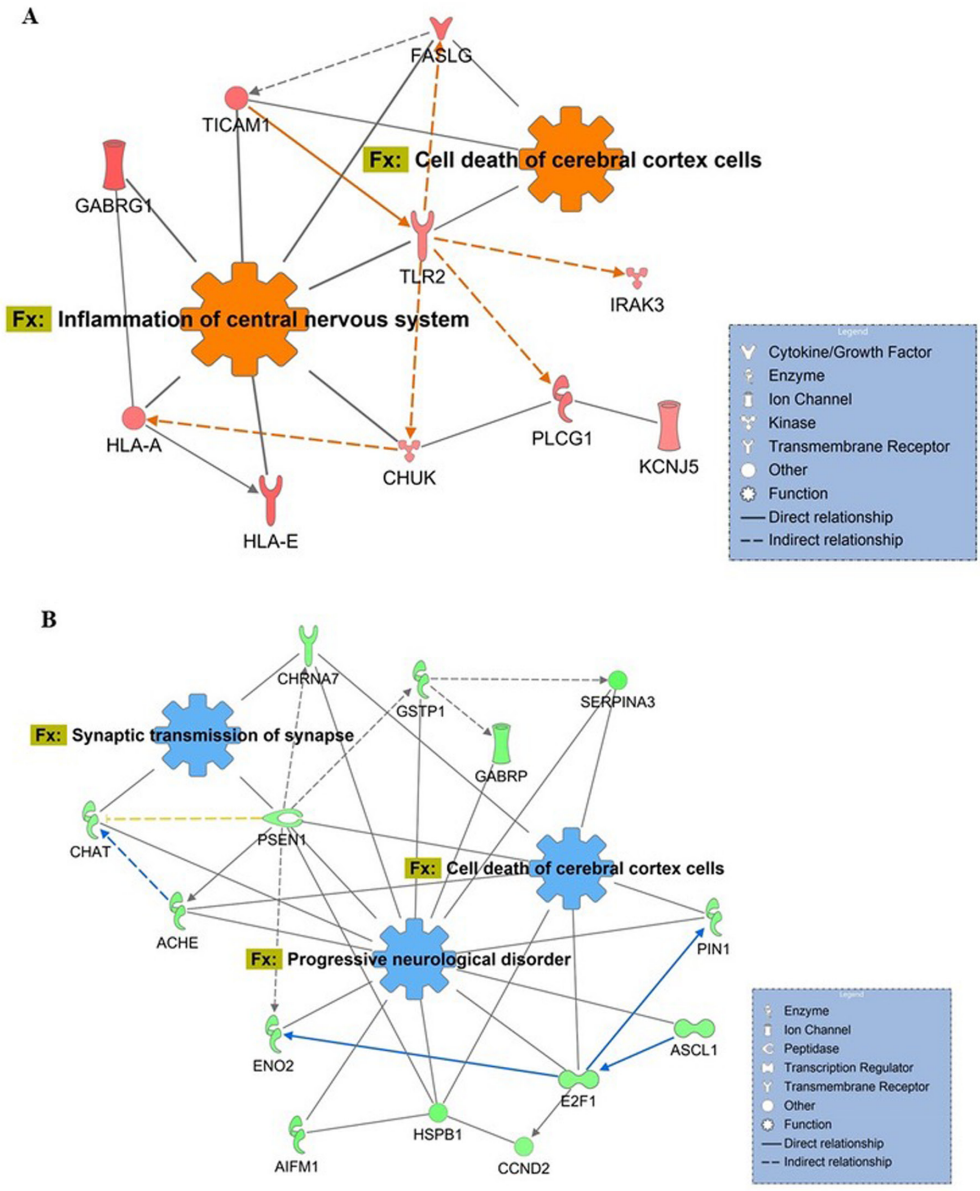

Fig. 4. A gene network map illustrating the interactions with a focus on neural functions in the cortex. (**A**) Interaction network of genes up-regulated by clothianidin (CLO) administration. (**B**) Interaction network of genes down-regulated by CLO administration.

well as *CHRNA7*, which synthesizes subunit α7 of nAChR, were decreased, suggesting that repeated exposure to CLO disrupts nAChR-mediated neurotransmission. In L2/3 of S1, only interneurons had α7 nAChRs, and *GABRP*, which synthesizes GABA receptor subunits, was also decreased, suggesting that repeated exposure to CLO overactivated pyramidal neurons by inhibiting the activity of interneurons. Since genetic variants in *PSEN1* and *SERPINA3* are involved in the pathogenesis of Alzheimer's disease [2, 18], a reduction of *PSEN1* and *SERPINA3* like that observed in this study may cause cognitive decline. In fact, it has been shown that spatial learning memory and object recognition memory are impaired in the Barnes maze test and the novel object recognition test in CLO-treated mice (in preparation for submission). This study is the first report of the neuronal effects of repeated exposure of mice to non-toxic doses of CLO followed over time using two-photon microscopy. The results suggested that CLO inhibited nAChR-bearing interneurons in the L2/3 of S1, leading to overactivation of neural circuits. It was also proposed that repeated exposure to CLO can cause inflammation in the brain. The present results provided new insights for understanding the mechanisms of neurobehavioral effects of NNs.

CONFLICT OF INTEREST. The authors declare that there are no conflicts of interest.

ACKNOWLEDGMENTS. This work was supported in part by Grants-in-Aid for Scientific Research A (JP18H04132: YI), B (JP19H04277: NH), and C (JP20K12619: YT), a Grant-in-Aid for Challenging Exploratory Research (JP21K19846: NH), a Grant-in-Aid for Early-Career Scientists (JP19K19406: TH), and a grant for Academic Transformation Area Research A (JP 20H05899: HW) from the Ministry of Education, Culture, Sports, Science and Technology of Japan. We also acknowledge financial support in the form of "Act Beyond Trust" (GIA) civil grants in 2020 and 2021 (NH). The funders had no role in the study design, data collection and analysis, decision to publish, or preparation of the manuscript.

REFERENCES

1. Akiyoshi, R., Wake, H., Kato, D., Horiuchi, H., Ono, R., Ikegami, A., Haruwaka, K., Omori, T., Tachibana, Y., Moorhouse, A. J. and Nabekura, J. 2018. Microglia enhance synapse activity to promote local network synchronization. *eNeuro* **5**: ENEURO.0088-18.
2. Akbor, M. M., Kurosawa, N., Nakayama, H., Nakatani, A., Tomobe, K., Chiba, Y., Ueno, M., Tanaka, M., Nomura, Y. and Isobe, M. 2021. Polymorphic SERPINA3 prolongs oligomeric state of amyloid beta. *PLoS One* **16**: e0248027. [Medline] [CrossRef]
3. Bouchard, M. F., Bellinger, D. C., Wright, R. O. and Weisskopf, M. G. 2010. Attention-deficit/hyperactivity disorder and urinary metabolites of organophosphate pesticides. *Pediatrics* **125**: e1270–e1277. [Medline] [CrossRef]
4. Chao, S. L. and Casida, J. E. 1997. Interaction of imidacloprid metabolites and analogs with the nicotinic acetylcholine receptor of mouse brain in relation to toxicity. *Pestic. Biochem. Physiol.* **58**: 77–88. [CrossRef]
5. Chen, D., Liu, Z., Barrett, H., Han, J., Lv, B., Li, Y., Li, J., Zhao, Y. and Wu, Y. 2020. Nationwide biomonitoring of neonicotinoid insecticides in breast milk and health risk assessment to nursing infants in the Chinese population. *J. Agric. Food Chem.* **68**: 13906–13915. [Medline] [CrossRef]
6. Dwyer, J. B., McQuown, S. C. and Leslie, F. M. 2009. The dynamic effects of nicotine on the developing brain. *Pharmacol. Ther.* **122**: 125–139. [Medline] [CrossRef]
7. Farag, M. R., Abou-El, F. M. F., EL-Sayed, G. G. and EL-Sayed, E. W. 2019. Modulatory effect of ginger aqueous extract against imidacloprid-induced neurotoxicity in rats. *Zag. Vet. J.* **47**: 432–446. [CrossRef]
8. Faro, L. R., Oliveira, I. M., Durán, R. and Alfonso, M. 2012. *In vivo* neurochemical characterization of clothianidin induced striatal dopamine release. *Toxicology* **302**: 197–202. [Medline] [CrossRef]
9. Food and Agriculture Organization of the United Nations. 2011. FAO Specifications and Evaluations for Agricultural Pesticide Clothianidin. http://www.fao.org/fileadmin/templates/agphome/documents/Pests_Pesticides/Specs/Clothianidin2011.pdf [accessed on January 10, 2020].
10. Hirano, T., Yanai, S., Omotehara, T., Hashimoto, R., Umemura, Y., Kubota, N., Minami, K., Nagahara, D., Matsuo, E., Aihara, Y., Shinohara, R., Furuyashiki, T., Mantani, Y., Yokoyama, T., Kitagawa, H. and Hoshi, N. 2015. The combined effect of clothianidin and environmental stress on the behavioral and reproductive function in male mice. *J. Vet. Med. Sci.* **77**: 1207–1215. [Medline] [CrossRef]
11. Hirano, T., Yanai, S., Takada, T., Yoneda, N., Omotehara, T., Kubota, N., Minami, K., Yamamoto, A., Mantani, Y., Yokoyama, T., Kitagawa, H. and Hoshi, N. 2018. NOAEL-dose of a neonicotinoid pesticide, clothianidin, acutely induce anxiety-related behavior with human-audible vocalizations in male mice in a novel environment. *Toxicol. Lett.* **282**: 57–63. [Medline] [CrossRef]
12. Hirano, T., Miyata, Y., Kubo, S., Ohno, S., Onaru, K., Maeda, M., Kitauchi, S., Nishi, M., Tabuchi, Y., Ikenaka, Y., Ichise, T., Nakayama, S. M. M., Ishizuka, M., Arizono, K., Takahashi, K., Kato, K., Mantani, Y., Yokoyama, T. and Hoshi, N. 2021. Aging-related changes in the sensitivity of behavioral effects of the neonicotinoid pesticide clothianidin in male mice. *Toxicol. Lett.* **342**: 95–103. [Medline] [CrossRef]
13. Hoshi, N. 2021. Adverse effects of pesticides on regional biodiversity and their mechanisms. pp. 235–247. In: Risks and Regulation of New Technologies (Matsuda, T., Wolff, J. and Yanagawa, T. eds.), Springer, Singapore.
14. Ichikawa, G., Kuribayashi, R., Ikenaka, Y., Ichise, T., Nakayama, S. M. M., Ishizuka, M., Taira, K., Fujioka, K., Sairenchi, T., Kobashi, G., Bonmatin, J. M. and Yoshihara, S. 2019. LC-ESI/MS/MS analysis of neonicotinoids in urine of very low birth weight infants at birth. *PLoS One* **14**: e0219208. [Medline] [CrossRef]
15. Ikenaka, Y., Miyabara, Y., Ichise, T., Nakayama, S., Nimako, C., Ishizuka, M. and Tohyama, C. 2019. Exposures of children to neonicotinoids in pine wilt disease control areas. *Environ. Toxicol. Chem.* **38**: 71–79. [Medline]
16. Kimura-Kuroda, J., Komuta, Y., Kuroda, Y., Hayashi, M. and Kawano, H. 2012. Nicotine-like effects of the neonicotinoid insecticides acetamiprid and imidacloprid on cerebellar neurons from neonatal rats. *PLoS One* **7**: e32432. [Medline] [CrossRef]
17. Koukouli, F., Rooy, M., Tziotis, D., Sailor, K. A., O'Neill, H. C., Levenga, J., Witte, M., Nilges, M., Changeux, J. P., Hoeffer, C. A., Stitzel, J. A., Gutkin, B. S., DiGregorio, D. A. and Maskos, U. 2017. Nicotine reverses hypofrontality in animal models of addiction and schizophrenia. *Nat. Med.* **23**: 347–354. [Medline] [CrossRef]
18. Lanoiselée, H. M., Nicolas, G., Wallon, D., Rovelet-Lecrux, A., Lacour, M., Rousseau, S., Richard, A. C., Pasquier, F., Rollin-Sillaire, A., Martinaud, O., Quillard-Muraine, M., de la Sayette, V., Boutoleau-Bretonniere, C., Etcharry-Bouyx, F., Chauviré, V., Sarazin, M., le Ber, I., Epelbaum, S., Jonveaux, T., Rouaud, O., Ceccaldi, M., Félician, O., Godefroy, O., Formaglio, M., Croisile, B., Auriacombe, S., Chamard, L.,

Vincent, J. L., Sauvée, M., Marelli-Tosi, C., Gabelle, A., Ozsancak, C., Pariente, J., Paquet, C., Hannequin, D., Campion D., Collaborators of the CNR-MAJ Project. 2017. *APP, PSEN1*, and *PSEN2* mutations in early-onset Alzheimer disease: A genetic screening study of familial and sporadic cases. *PLoS Med.* **14**: e1002270. [Medline] [CrossRef]
19. Levin, E. D. and Simon, B. B. 1998. Nicotinic acetylcholine involvement in cognitive function in animals. *Psychopharmacology (Berl.)* **138**: 217–230. [Medline] [CrossRef]
20. Maeda, M., Kitauchi, S., Hirano, T., Ikenaka, Y., Nishi, M., Shoda, A., Murata, M., Mantani, Y., Tabuchi, Y., Yokoyama, T. and Hoshi, N. 2021. Fetal and lactational exposure to the no-observed-adverse-effect level (NOAEL) dose of the neonicotinoid pesticide clothianidin inhibits neurogenesis and induces different behavioral abnormalities at the developmental stages in male mice. *J. Vet. Med. Sci.* **83**: 542–548. [Medline] [CrossRef]
21. Masamizu, Y., Tanaka, Y. R., Tanaka, Y. H., Hira, R., Ohkubo, F., Kitamura, K., Isomura, Y., Okada, T. and Matsuzaki, M. 2014. Two distinct layer-specific dynamics of cortical ensembles during learning of a motor task. *Nat. Neurosci.* **17**: 987–994. [Medline] [CrossRef]
22. Nabekura, J. and Eto, K. 2010. In vivo imaging of the brain by two-photon laser microscopy. *Nippon Yakurigaku Zasshi* **135**: 104–108 (in Japanese). [Medline] [CrossRef]
23. Namba, K. and Ishihara, Y. 2021. Decreases in microglial activity and abnormal behaviors induced by developmental exposure to neonicotinoids. *48th Annu. Meeting Jpn. Sci. Toxicol*. P-86S.
24. Nie, X., Kitaoka, S., Tanaka, K., Segi-Nishida, E., Imoto, Y., Ogawa, A., Nakano, F., Tomohiro, A., Nakayama, K., Taniguchi, M., Mimori-Kiyosue, Y., Kakizuka, A., Narumiya, S. and Furuyashiki, T. 2018. The innate immune receptors TLR2/4 mediate repeated social defeat stress-induced social avoidance through prefrontal microglial activation. *Neuron* **99**: 464–479.e7. [Medline] [CrossRef]
25. Ohno, S., Ikenaka, Y., Onaru, K., Kubo, S., Sakata, N., Hirano, T., Mantani, Y., Yokoyama, T., Takahashi, K., Kato, K., Arizono, K., Ichise, T., Nakayama, S. M. M., Ishizuka, M. and Hoshi, N. 2020. Quantitative elucidation of maternal-to-fetal transfer of neonicotinoid pesticide clothianidin and its metabolites in mice. *Toxicol. Lett.* **322**: 32–38. [Medline] [CrossRef]
26. Okada, T., Kato, D., Nomura, Y., Obata, N., Quan, X., Morinaga, A., Yano, H., Guo, Z., Aoyama, Y., Tachibana, Y., Moorhouse, A. J., Matoba, O., Takiguchi, T., Mizobuchi, S. and Wake, H. 2021. Pain induces stable, active microcircuits in the somatosensory cortex that provide a therapeutic target. *Sci. Adv.* **7:** Eabd8261.
27. Oulhote, Y. and Bouchard, M. F. 2013. Urinary metabolites of organophosphate and pyrethroid pesticides and behavioral problems in Canadian children. *Environ. Health Perspect.* **121**: 1378–1384. [Medline] [CrossRef]
28. Oya, N., Ito, Y., Ebara, T., Kato, S., Ueyama, J., Aoi, A., Nomasa, K., Sato, H., Matsuki, T., Sugiura-Ogasawara, M., Saitoh, S. and Kamijima, M. 2021. Cumulative exposure assessment of neonicotinoids and an investigation into their intake-related factors in young children in Japan. *Sci. Total Environ.* **750**: 141630. [Medline] [CrossRef]
29. Pentel, P. R., Keyler, D. E., Chen, Y., LeSage, M. G., Dufek, M. B., Le, C. and Leslie, F. M. 2006. Vaccination against nicotine does not prevent nicotine-induced changes in fetal nicotinic receptor binding and c-fos mRNA expression in rats. *Neurotoxicol. Teratol.* **28**: 589–596. [Medline] [CrossRef]
30. Picciotto, M. R., Brunzell, D. H. and Caldarone, B. J. 2002. Effect of nicotine and nicotinic receptors on anxiety and depression. *Neuroreport* **13**: 1097–1106. [Medline] [CrossRef]
31. Poorthuis, R. B., Bloem, B., Verhoog, M. B. and Mansvelder, H. D. 2013. Layer-specific interference with cholinergic signaling in the prefrontal cortex by smoking concentrations of nicotine. *J. Neurosci.* **33**: 4843–4853. [Medline] [CrossRef]
32. Simon-Delso, N., Amaral-Rogers, V., Belzunces, L. P., Bonmatin, J. M., Chagnon, M., Downs, C., Furlan, L., Gibbons, D. W., Giorio, C., Girolami, V., Goulson, D., Kreutzweiser, D. P., Krupke, C. H., Liess, M., Long, E., McField, M., Mineau, P., Mitchell, E. A., Morrissey, C. A., Noome, D. A., Pisa, L., Settele, J., Stark, J. D., Tapparo, A., Van Dyck, H., Van Praagh, J., Van der Sluijs, J. P., Whitehorn, P. R. and Wiemers, M. 2015. Systemic insecticides (neonicotinoids and fipronil): trends, uses, mode of action and metabolites. *Environ. Sci. Pollut. Res. Int.* **22**: 5–34. [Medline] [CrossRef]
33. Takada, T., Yoneda, N., Hirano, T., Onaru, K., Mantani, Y., Yokoyama, T., Kitagawa, H., Tabuchi, Y., Nimako, C., Ishizuka, M., Ikenaka, Y. and Hoshi, N. 2020. Combined exposure to dinotefuran and chronic mild stress counteracts the change of the emotional and monoaminergic neuronal activity induced by either exposure singly despite corticosterone elevation in mice. *J. Vet. Med. Sci.* **82**: 350–359. [Medline] [CrossRef]
34. Takada, T., Yoneda, N., Hirano, T., Yanai, S., Yamamoto, A., Mantani, Y., Yokoyama, T., Kitagawa, H., Tabuchi, Y. and Hoshi, N. 2018. Verification of the causal relationship between subchronic exposures to dinotefuran and depression-related phenotype in juvenile mice. *J. Vet. Med. Sci.* **80**: 720–724. [Medline] [CrossRef]
35. Thévenaz, P., Ruttimann, U. E. and Unser, M. 1998. A pyramid approach to subpixel registration based on intensity. *IEEE Trans. Image Process.* **7**: 27–41. [Medline] [CrossRef]
36. Tomizawa, M. and Casida, J. E. 2002. Desnitro-imidacloprid activates the extracellular signal-regulated kinase cascade via the nicotinic receptor and intracellular calcium mobilization in N1E-115 cells. *Toxicol. Appl. Pharmacol.* **184**: 180–186. [Medline] [CrossRef]
37. Tomizawa, M. and Casida, J. E. 2005. Neonicotinoid insecticide toxicology: mechanisms of selective action. *Annu. Rev. Pharmacol. Toxicol.* **45**: 247–268. [Medline] [CrossRef]
38. Ueyama, J., Harada, K. H., Koizumi, A., Sugiura, Y., Kondo, T., Saito, I. and Kamijima, M. 2015. Temporal levels of urinary neonicotinoid and dialkylphosphate concentrations in Japanese women between 1994 and 2011. *Environ. Sci. Technol.* **49**: 14522–14528. [Medline] [CrossRef]
39. Yoneda, N., Takada, T., Hirano, T., Yanai, S., Yamamoto, A., Mantani, Y., Yokoyama, T., Kitagawa, H., Tabuchi, Y. and Hoshi, N. 2018. Peripubertal exposure to the neonicotinoid pesticide dinotefuran affects dopaminergic neurons and causes hyperactivity in male mice. *J. Vet. Med. Sci.* **80**: 634–637. [Medline] [CrossRef]